Investigation of the processes for reversible hydrogen storage in the Li–Mg–N–H system

Raphaël Janot [*], Jean-Bruno Eymery, Jean-Marie Tarascon

Laboratoire de Réactivité et Chimie des Solides, UMR 6007-CNRS, Université de Picardie, Jules Verne, 33 rue St Leu, 80039 Amiens Cedex, France

Abstract

The hydrogen storage performances of the Li–Mg–N–H system are investigated starting either from 1:2 $Mg(NH_2)_2$–LiH or 1:2 MgH_2–$LiNH_2$ ball-milled mixtures. It is shown that, for 1:2 MgH_2–$LiNH_2$, an ammonia release occurs if the first heating is conducted under a dynamic vacuum, leading to a fast degradation of the material. The positive role of LiH, if initially present in the mixture, is therefore emphasized as LiH rapidly reacts with ammonia and avoids the contamination of the hydrogen desorbing flow. The desorption kinetics of the ball-milled 1:2 $Mg(NH_2)_2$–LiH mixture are fast: a total amount of 5.0 wt.% of hydrogen is desorbed in 25 min at 220 °C. This material exhibits a nice reversibility at 200 °C with an experimental capacity around 4.8 wt.%. Preliminary results are given on the structure of $Li_2Mg(NH)_2$, formed upon desorption: this phase crystallizes in a cubic unit cell with a lattice parameter of 10.06(1) Å. In addition, by plotting an absorption isotherm of the $Li_2Mg(NH)_2$ phase at 200 °C, two pressure plateaus are observed revealing the existence of an intermediary phase between $Li_2Mg(NH)_2$ and the rehydrided material, which is the 1:2 $Mg(NH_2)_2$–LiH mixture.
© 2006 Elsevier B.V. All rights reserved.

Keywords: Hydrogen storage; Imides; Amides; Ammonia; Ball-milling

1. Introduction

Safe hydrogen storage remains a great challenge for the development of fuel cell technologies in the field of vehicular applications. Due to safety problems encountered with conventional techniques (cryogenic or compressed gas), the use of solid-state materials, which reversibly absorb (or adsorb) hydrogen is promising, but the research for the elaboration of new compounds with both a high capacity and a fast hydrogen release at low temperature is still tremendous. Indeed, many metals or alloys readily absorb hydrogen, even at room temperature, but their gravimetric hydrogen capacity is limited to about 1.5 wt.% [1,2], a value far from that desired for on-board hydrogen storage. Magnesium exhibits a much higher capacity (7.6 wt.% based on the formation of MgH_2), but the sorption kinetics are slow and a temperature of 350 °C is required to reach a 1 bar equilibrium hydrogen pressure [3].

Complex hydrides (combining both covalent and ionic bonds) gained a lot of attention in the last years, due to their high capacities at moderate temperature (below 200 °C). The most investigated complex hydride is sodium alanate ($NaAlH_4$) with a theoretical capacity of 5.6 wt.%, and for which a partial reversibility is achieved by the addition of various Ti-based catalysts [4,5]. However, due to slow reaction kinetics and a limited reversibility (3.6 wt.% at 150 °C, as the reaction between $NaAlH_4$ and Na_3AlH_6 is the only viable for practical applications), $NaAlH_4$ is not completely satisfactory for mobile applications.

Metal–N–H systems have recently appeared as new promising materials for reversible hydrogen storage [6]. Lithium nitride was shown to react with hydrogen following a two-step process leading to the successive formations of lithium imide (Li_2NH) and lithium amide ($LiNH_2$) [7]. As the enthalpy of the first step is strongly negative (e.g. the equilibrium hydrogen pressure is very low: about 0.01 bar at 280 °C), only the second step is practically available. A capacity of 6.5 wt.% is stored following the reaction: $Li_2NH + H_2 \leftrightarrow LiNH_2 + LiH$, but a temperature as high as 280 °C is needed to obtain a 1 bar hydrogen pressure [8,9]. Many studies have been devoted to the destabilization of the Li–N–H

* Corresponding author. Tel.: +33 3 22 82 79 01; fax: +33 3 22 82 75 90.
  E-mail address: raphael.janot@sc.u-picardie.fr (R. Janot).

system by the partial substitution of Li for other elements. Among them, the substitution by Mg appears very promising as it significantly decreases the enthalpy of the reaction, and thus favours reversible hydrogen storage near ambient conditions.

Studies on various Mg:Li ratios have been reported in the literature and can be resumed as follows:

- Mg:Li = 1:2 (cf. Luo and Sickafoose [10,11], Chen and co-workers [12,13])

$$3Mg(NH_2)_2 + 6LiH \leftrightarrow 3Li_2Mg(NH)_2 + 6H_2 \quad (1)$$

- Mg:Li = 3:8 (cf. Fujii and co-workers [14,15])

$$3Mg(NH_2)_2 + 8LiH \leftrightarrow 4Li_2NH + Mg_3N_2 + 8H_2 \quad (2)$$

- Mg:Li = 1:4 (cf. Orimo et al. [16,17])

$$3Mg(NH_2)_2 + 12LiH \leftrightarrow 4Li_3N + Mg_3N_2 + 12H_2 \quad (3)$$

The trend is that the reversible capacity increases when decreasing the Mg content. The capacity reaches 7.0 and 9.2 wt.% for reactions (2) and (3), but a high temperature (up to 500 °C) is required to achieve a full hydrogen desorption for these reactions, due to the stability of the transitory imide phases. Consequently, the most promising material concerns Mg:Li = 1:2 ratio, with both a high capacity (5.6 wt.%) and a relatively low operating temperature (about 200 °C). The present paper deals with the investigation of that system involving the formation of the new ternary $Li_2Mg(NH)_2$ imide.

The $Li_2Mg(NH)_2$ imide can be prepared starting from both 1:2 $Mg(NH_2)_2$–LiH and 1:2 MgH_2–$LiNH_2$ mixtures. The difference in desorption mechanisms will be discussed in this paper owing to the investigations made by X-ray diffraction, infrared spectroscopy, temperature-programmed-desorption coupled with a mass spectrometer (TPD-MS) and gravimetric measurements. The importance of the recombination process of ammonia (obtained by decomposition of amide upon heating) with the hydride to produce hydrogen will be emphasized.

2. Experimental

2.1. Samples preparation

Commercial powders are used for LiH (Aldrich, 95%, 40 μm), $LiNH_2$ (Aldrich, 95%) and MgH_2 (Goldschmidt, 95%). $Mg(NH_2)_2$ is prepared by ball-milling commercial MgH_2 under ammonia for 12 h. The synthesis of pure magnesium amide is checked by X-ray diffraction (no trace of remaining Mg or MgH_2) and infrared spectroscopy (NH stretching bands at 3275 and 3330 cm^{-1}).

The 1:2 $Mg(NH_2)_2$–LiH and 1:2 MgH_2–$LiNH_2$ mixtures are prepared by ball-milling under argon the different phases, using a Retsch PM100 miller equipped with stainless steel tools (container with a 50 cm^3 internal volume and balls with a 10 mm diameter). The ball to powder weights ratio is fixed at 40:1. A typical synthesis concerns 2 g of powders milled at 600 rpm for 12 h. Upon milling, a period of 5 min rest is performed every

30 min in order to limit the temperature increase, and to avoid the decomposition of the powders. The entire handling of the reactants and products is carried out in a glove box with a circulation of purified argon.

2.2. Characterizations

The structural determination is performed using a Scintag powder diffractometer with Cu Kα_{1+2} radiation ($\lambda = 1.5418$ Å). The step increment is 0.02° measured during 1 s. Due to the high reactivity of the ball-milled mixtures with moisture, an air-tightened sample holder with a beryllium window was used. This device is responsible for the presence of Be sharp reflections on the XRD patterns ($2\theta = 45.8, 50.9, 52.8$ and $70.9°$).

The infrared spectroscopy is a powerful technique for the distinction between amide and imide, as these compounds are well characterized by the vibrations bands of their covalent N–H bonds. The present study is made by mixing the sample (around 2 wt.% in weight) with KBr powder. The mixture is then pressed at 8 tonnes to form a pellet (13 mm in diameter). The data collection is achieved in the transmission mode using a Nicolet Avatar 370 DTGS infrared spectrometer.

TPD experiments (temperature-programmed-desorption coupled with a mass spectrometer) are conducted to obtain a fast determination of the temperature of hydrogen release for the various samples. This technique allows also the visualization of the possible evolution of ammonia upon heating. In addition, the activation energy of desorption process is calculated using the Kissinger's law from the desorption curves obtained at different heating rates. This study is managed with a quadrupolar mass spectrometer QXK300 (VG Scientific Ltd.). The procedure consists in putting about 5 mg of powder in a stainless steel tube (6 mm in diameter). This tube is then connected to the mass spectrometer and outgases under a primary vacuum (10^{-2} mbar). The TPD curves are acquired at heating rates ranging from 1 to 20 °C min^{-1} and temperatures up to 600 °C.

The hydrogen storage performances are determined by both gravimetric and volumetric measurements.

- The gravimetric study is managed with a Hiden IGA001 apparatus (an "Intelligent Gravimetric Analyser" especially designed for the monitoring of gas sorption on solid materials) equipped with an antechamber allowing the loading of the sample without any air exposure. A typical 100 mg sample weight is loaded into a stainless steel bucket and then outgased under a primary vacuum (10^{-2} mbar) for 2 h at room temperature before each experiment. The sample weight is then continuously monitored upon hydrogen absorption–desorption at a given temperature.
- The volumetric measurement is made using a Sievert-type instrument designed in our laboratory. The sample is transferred in the glove box into a stainless steel capillary and the capillary is then connected to Sievert's apparatus. After outgasing at room temperature, the hydrogen absorption/desorption properties of the sample can be calculated from the pressure changes in calibrated volumes using the ideal gas law.

For both techniques, high purity hydrogen (Air Liquide, 99.999%) is used. The hydrogen contents, reported in the paper, are given as weight percents of the whole sample including inactive components (such as catalysts).

3. Results and discussion

3.1. Transformation between 1:2 MgH_2–$LiNH_2$ and 1:2 $Mg(NH_2)_2$–LiH

Fig. 1 presents the evolution of the XRD diagrams of the 1:2 MgH_2–$LiNH_2$ mixture upon ball-milling, heating under vacuum and rehydrogenation, successively. The XRD pattern of the starting mixture (Fig. 1a) reveals that a small amount of free Mg is present in commercial MgH_2. Its amount is estimated at 5 wt.% of the total weight of MgH_2. All other reflections can be indexed in the tetragonal unit cells of $LiNH_2$ (space group *I*-4) and MgH_2 (space group $P4_2/mnm$). After 12 h of ball-milling only broad reflections are observed (Fig. 1b) indicating a strong amorphization and/or a decrease in the particles size. After 2 h of desorption under a primary vacuum at 200 °C of the ball-milled mixture, new reflections appear (Fig. 1c). These peaks are assigned to the formation of the ternary imide $Li_2Mg(NH)_2$ and are in good agreement with the recently reported patterns [12,13]. The structure of this new phase will be discussed below in a specific paragraph. The hydrogenation under 100 bar at 200 °C of the $Li_2Mg(NH)_2$ compound leads to the formation of $Mg(NH_2)_2$ and LiH. On the XRD diagram (Fig. 1d), all the sharp reflections can be indexed in the tetragonal unit cell of $Mg(NH_2)_2$ (space group $I4_1/acd$). The presence of LiH is not detected by XRD probably due to the highly divided state of the material and its low number of electrons.

In addition to XRD, the structural changes are also identified by infrared spectroscopy as shown in Fig. 2. The $LiNH_2$ spectrum exhibits characteristic NH bands at 3255 and 3310 cm^{-1}, symmetric and asymmetric stretching [18], respectively (Fig. 2a). This study confirms that $LiNH_2$ is not decomposed upon ball-milling, since these NH stretching bands
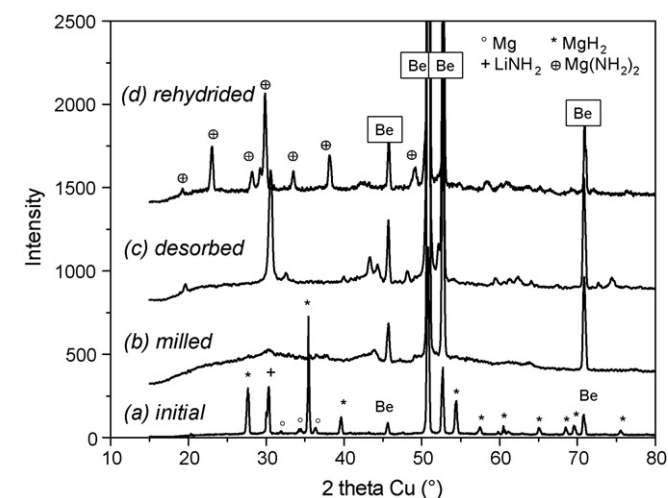
Fig. 1. X-ray diagrams of 1:2 MgH_2–$LiNH_2$: initial mixture (a), 12 h ball-milled (b), desorbed at 200 °C (c) and rehydrogenated under 100 bar at 200 °C (d).
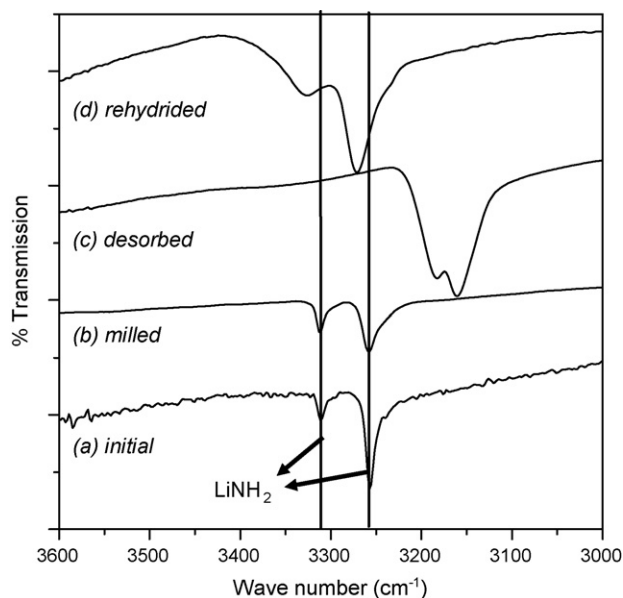
Fig. 2. Infrared spectra of 1:2 MgH_2–$LiNH_2$: initial mixture (a), 12 h ball-milled (b), desorbed at 200 °C (c) and rehydrogenated under 100 bar at 200 °C (d).

are still visible in Fig. 2b. The 5-min rest performed every 30 min during the milling strongly limits the temperature increase of the powders and avoids the transformation of $LiNH_2$ into Li_2NH. After heating under vacuum at 200 °C, two convoluted peaks at 3160 and 3182 cm^{-1} appear (Fig. 2c) and can be attributed to the $Li_2Mg(NH)_2$ imide. These wave numbers are slightly lower than those of Li_2NH (3185 cm^{-1} [19]) and MgNH (3195 cm^{-1} [20]). There are no bands with higher wave numbers left, suggesting that the conversion to imide is complete. The spectrum of Fig. 1d displays two NH stretching bands at 3275 and 3330 cm^{-1}, values close to those found in the literature for $Mg(NH_2)_2$ [20].

Both X-ray diffraction and IR spectroscopy show therefore that the rehydrided material in the Li–Mg–N–H system is the 1:2 $Mg(NH_2)_2$–LiH mixture and not 1:2 MgH_2–$LiNH_2$. We can also notice that a simple annealing under argon (100 bar, 200 °C) of 1:2 MgH_2–$LiNH_2$ leads to the same transformation, showing the higher thermodynamic stability of 1:2 $Mg(NH_2)_2$–LiH. The reaction responsible for reversible hydrogen storage in the Li–Mg–N–H system is therefore the following:

$$Mg(NH_2)_2 + 2LiH \leftrightarrow Li_2Mg(NH)_2 + 2H_2 \quad (4)$$
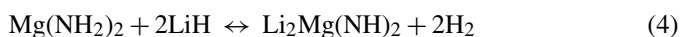
3.2. Structure of $Li_2Mg(NH)_2$

Since the early work of Luo [10], several studies have confirmed the existence of a ternary $Li_2Mg(NH)_2$ imide, but its structure remains unknown. In this paper, we try to bring some preliminary data on the crystallographic unit cell of this material. Fig. 3 gives the XRD pattern of a powder obtained after heating under primary vacuum for 12 h at 200 °C. Actually, all the reflections are indexable in a cubic unit cell with a lattice parameter of 10.06(1) Å. The structure is closely related to the antifluorite type, as many other amides and imides with alkali metals. The nitrogen atoms form a face-centred-cubic unit cell and the metallic cations partially occupy the tetrahedral sites.
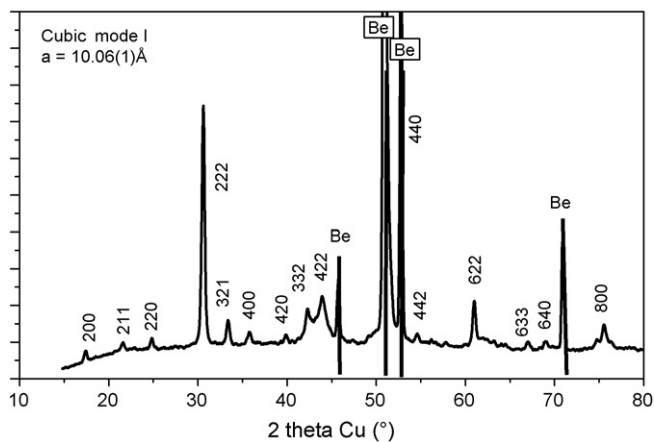
Fig. 3. X-ray diagram of $Li_2Mg(NH)_2$. Indexation in a cubic unit cell. Mode I, $a = 10.06(1)$ Å.

Fig. 4. TPD spectrum of 12 h ball-milled 1:2 MgH_2–$LiNH_2$ recorded at a heating rate of $10\,^{\circ}C\,min^{-1}$. Desorption curves for hydrogen (solid line) and ammonia (dotted line).

Whereas, in Li_2NH, all the tetrahedral sites are filled with Li [21], here the Li and Mg atoms occupy only 3/4 of the vacant sites, in a similar structure as that of Mg_3N_2.

For one basic antifluorite unit cell containing eight tetrahedral sites, we have two Mg atoms, four Li atoms and two sites remaining unoccupied. A periodic arrangement of the vacancies leads to a sur-structure with a lattice parameter twice that of the elemental unit cell. The unit cell of the $Li_2Mg(NH)_2$ phase is therefore composed of eight elemental antifluorite unit cells with 3/4 of the tetrahedral sites being occupied. The calculated density from these crystallographic data is 1.78, a value close to the one experimentally measured by liquid pycnometry (1.68).

The best fit of the experimental diagram is obtained when the Li and Mg atoms randomly occupy the tetrahedral sites. As soon as a structural order between the Li and Mg atoms is fixed, the calculated intensities of the reflections, especially the (2 1 1) line, do not fit so well with the experimental diagram. Further experiments are in progress to fully resolve the structure. Neutron diffraction on a deuterated compound will be especially carried out to determine the positions of the hydrogen atoms, and try to find the space group of this compound.

3.3. Comparison of the first desorption of 1:2 MgH_2–$LiNH_2$ and 1:2 $Mg(NH_2)_2$–LiH

The 1:2 $Mg(NH_2)_2$–LiH and 1:2 MgH_2–$LiNH_2$ mixtures are both prepared by 12 h ball-milling. Fig. 4 exhibits a typical TPD curve, obtained at a heating rate of $10\,^{\circ}C\,min^{-1}$, whatever the starting composition. After 12 h of ball-milling, one strong hydrogen desorption peak is observed: the hydrogen desorption starts at about $140\,^{\circ}C$ and reaches its maximum at $192\,^{\circ}C$. The peak of hydrogen release is narrow emphasizing the good homogeneity of the ball-milled powders. The hydrogen desorption occurs at a temperature much lower than the decomposition temperatures of the single constituent phases. Using the same experimental features, the hydrogen desorption proceeds at $450\,^{\circ}C$ for MgH_2 and more than $600\,^{\circ}C$ for LiH. For the metallic amides, the ammonia releases are observed at about 350 and $400\,^{\circ}C$ for $Mg(NH_2)_2$ [16] and $LiNH_2$ [21], respectively. This
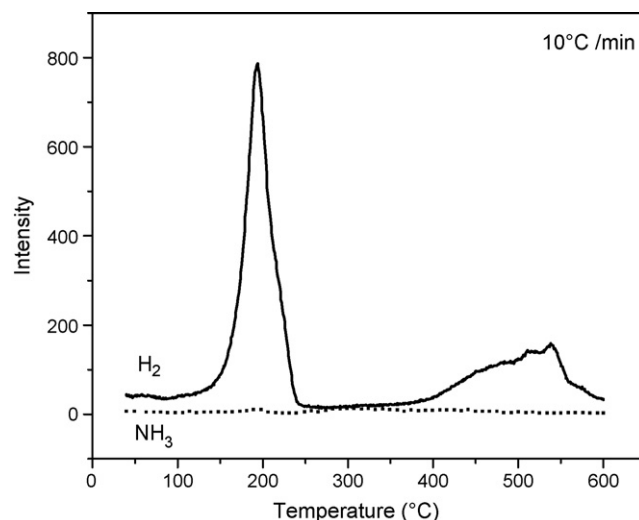
observation shows that a strong interaction lies between MgH_2 and $LiNH_2$ or $Mg(NH_2)_2$ and LiH, most likely due to the nanometric size of the 12 h ball-milled powders. Longer milling does not improve the mixing of the different phases and does not lead to a decrease in the hydrogen desorption temperature. In addition to the main peak at $192\,^{\circ}C$, hydrogen desorption is also observed at higher temperatures on the TPD curve of Fig. 4. This broad peak starts around $400\,^{\circ}C$ and reaches its maximum at $540\,^{\circ}C$. It is assigned to the decomposition of the $Li_2Mg(NH)_2$ phase leading to the formation of Li–Mg nitrides. Another important result is that no ammonia release is observed on the whole range of temperatures, for both 1:2 $Mg(NH_2)_2$–LiH and 1:2 MgH_2–$LiNH_2$ mixtures, as detected by TPD-MS.

After having demonstrated that the hydrogen desorption occurs below $200\,^{\circ}C$, the influence of the starting components on the kinetics of hydrogen release are now investigated by detailed gravimetric measurements. Fig. 5 shows the weight losses, at $200\,^{\circ}C$, of the 12 h ball-milled 1:2 MgH_2–$LiNH_2$ powder under different hydrogen pressures. Surprisingly, the weight loss under dynamic vacuum (around 10^{-2} mbar) exceeds the theoretical capacity (5.6 wt.% based on reaction (4)), reaching 8.4 wt.% after 180 min of pumping. A comparison can be made with the behaviour of 1:2 $Mg(NH_2)_2$–LiH, presented in Fig. 6, for which the weight loss reaches about 5.0 wt.% under the same experimental conditions ($200\,^{\circ}C$-primary vacuum). There is therefore a strong discrepancy between the first desorption runs of the 1:2 $Mg(NH_2)_2$–LiH and 1:2 MgH_2–$LiNH_2$ mixtures. It seems that, although no trace of ammonia is detected by TPD-MS, a slight ammonia release occurs when starting with 1:2 MgH_2–$LiNH_2$.

This can be explained if we assume that the hydrogen release proceeds by a two-step reaction similar to that encountered for the Li–N–H system. Indeed, Hu and Ruckenstein [22] have demonstrated that the hydrogen release from the 1:1 LiH–$LiNH_2$ mixture is mediated by ammonia and occurs via two successive solid–gas reactions, which are first, the decomposition of $LiNH_2$ leading to the formation of Li_2NH and NH_3 and, second, the
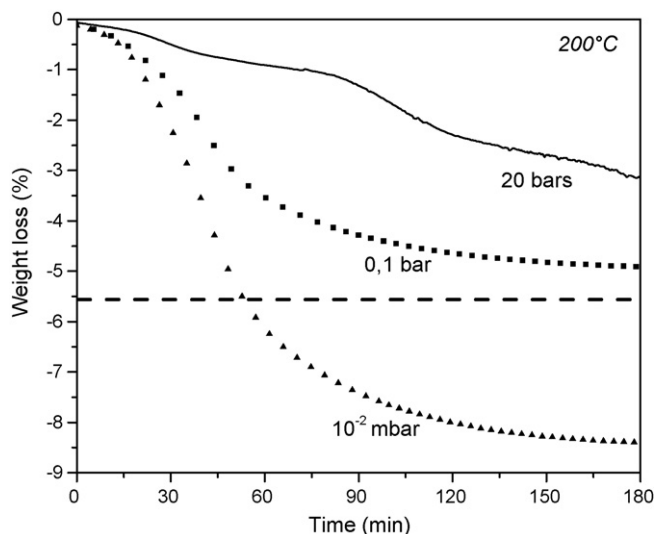
Fig. 5. Weight losses of 12 h ball-milled 1:2 MgH_2–$LiNH_2$ at 200 °C under various hydrogen pressures.

reaction of the evolving NH_3 with LiH to form H_2 and $LiNH_2$. Moreover, it has been shown that the second step, the reaction of LiH with NH_3, is very fast [22]. This prevents an ammonia contamination of the hydrogen desorbing flow and simply means that the kinetic of hydrogen desorption of the Li–N–H system is monitored by the decomposition rate of $LiNH_2$.

Following a similar process, we can write the following two reactions for the 1:2 MgH_2–$LiNH_2$ mixture:

$$2LiNH_2 \rightarrow Li_2NH + NH_3 \quad (5)$$

$$MgH_2 + 2NH_3 \rightarrow Mg(NH_2)_2 + 2H_2 \quad (6)$$
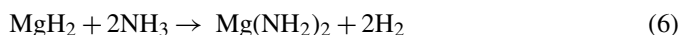
However, the reaction of MgH_2 with NH_3 is much slower than that of LiH. This is especially observed when preparing the Li and Mg amides from the corresponding hydrides by ball-milling under ammonia. A 30 min milling is sufficient for the completion
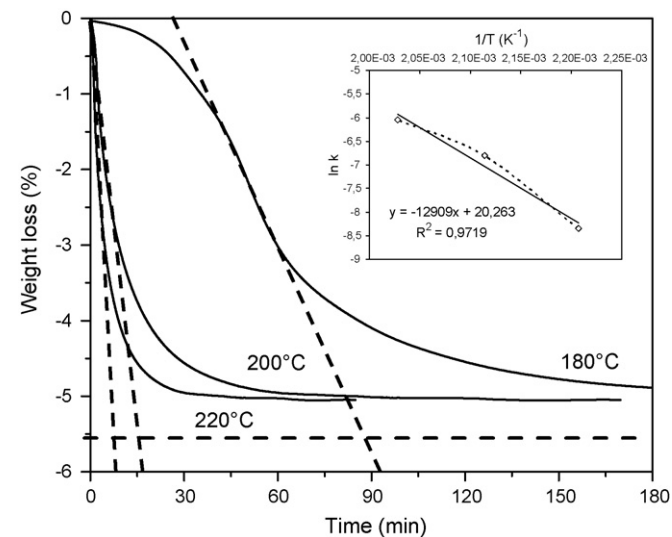
of the $LiNH_2$ synthesis, whereas 12 h are necessary to achieve the formation of pure $Mg(NH_2)_2$. This is simply due to the lower electronegativity of Li versus Mg giving a highly reducing character to LiH. As the reaction of MgH_2 with NH_3 (reaction (6)) is slow, a slight amount of ammonia can be released when desorption of the 1:2 MgH_2–$LiNH_2$ mixture is performed under dynamic vacuum. On the contrary, if the desorption is managed under a residual hydrogen pressure (for instance, 0.1 bar, as presented in Fig. 5), the weight loss is in good agreement with reaction (4), as it reaches 5.0 wt.% after 180 min. Even under a 20 bar hydrogen pressure, the 1:2 MgH_2–$LiNH_2$ mixture can desorb hydrogen, obviously with a slowing down kinetic, which shows that the equilibrium hydrogen pressure of the system is above 20 bar at 200 °C, as already reported [10].

For 1:2 $Mg(NH_2)_2$–LiH, the presence of LiH in the initial mixture enables to avoid the ammonia release as LiH reacts very quickly with NH_3 formed by the decomposition of $Mg(NH_2)_2$. Actually, LiH acts as ammonia getter and therefore enables to keep the integrity of the starting material and to have a better cyclability upon the following hydrogen absorption–desorption cycles.

3.4. Cycling of the 1:2 $Mg(NH_2)_2$–LiH mixture

Fig. 6 shows the kinetics of first desorption under primary vacuum, for the 1:2 $Mg(NH_2)_2$–LiH mixture, obtained at different temperatures (180, 200 and 220 °C). At 180 °C, the full desorption (around 5.1% of weight loss) occurs in 180 min of pumping. The desorption rates are much faster at 200 and 220 °C, since 60 and 25 min are sufficient for the achievement of the desorption process, making the 1:2 $Mg(NH_2)_2$–LiH system as one of the most performing materials with high storage capacities at these temperatures. The sole material with higher capacity, which is MgH_2 with 7.6 wt.% of reversible hydrogen storage, has a much slower desorption kinetic at 200 °C, even with catalysts addition [23,24].

The activation energy of desorption process is estimated by plotting the maximum reaction rate (k) as a function of the temperature (T). The reaction rates are obtained from the slopes of the tangents (drawn by dashed lines in Fig. 6) at the inflection points of the desorption curves. Fig. 6 insert exhibits the Arrhenius plot, where the activation energy is calculated by performing a linear regression of the ln k versus $1/T$ curve. A value of 107 kJ mol^{-1} is found, which is in very good agreement with that reported by Xiong et al. (102 kJ mol^{-1}) [13]. The activation energy is also determined using TPD-MS by plotting hydrogen desorption curves at various heating rates (cf. Fig. 7). Kissinger's method [25] is used for the calculation of the energy:

$$\frac{d(\ln \beta / T_m^2)}{d(1/T_m)} = \frac{-E_a}{R}$$

Here T_m is the temperature at which the hydrogen desorption reaches its peak on the TPD curve, β the heating rate, E_a the activation energy and R the gas constant. Fig. 7 insert, displays a linear plot of $\ln(\beta/T_m^2)$ versus $1/T_m$. The slope of the fitted line leads to a value for the activation energy of 111 kJ mol^{-1}, in good accordance with the energy obtained from the desorption

Fig. 6. Weight losses of 12 h ball-milled 1:2 $Mg(NH_2)_2$–LiH under primary vacuum at various temperatures. In insert, Arrhenius plot allowing the calculation of the activation energy.
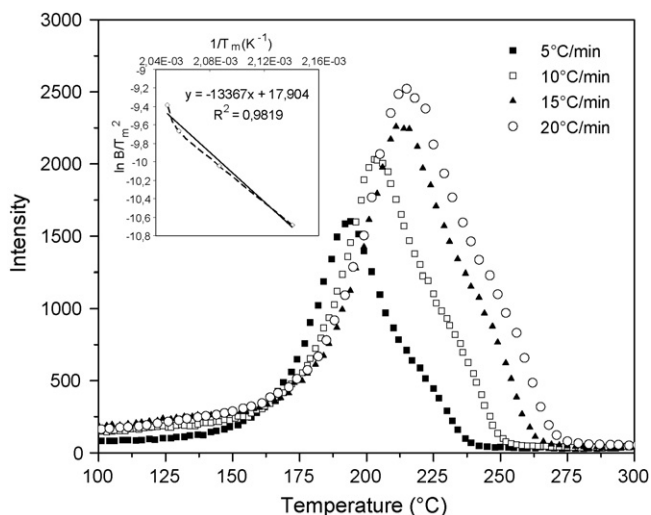
Fig. 7. TPD spectra of 12 h ball-milled 1:2 $Mg(NH_2)_2$–LiH recorded at various heating rates. In insert, Kissinger's plot allowing the calculation of the activation energy.

kinetics given in Fig. 6. We can notice that these values (in the range 102–111 kJ mol^{-1}) are lower than the activation energy of the desorption process of MgH_2 (120–142 kJ mol^{-1} [26]), partially explaining why the hydrogen release around 200 °C is faster for the Li–Mg–N–H system. Finally, we tried to decrease the value of the activation energy by adding various catalysts to the 1:2 $Mg(NH_2)_2$–LiH mixture (Pd nanoparticles, $TiCl_3$, Nb_2O_5). But, no significant result was obtained and, unfortunately, the desorption kinetics were not improved, conversely to some catalytic effects reported for the Li–N–H system [27,28]. This discrepancy is somewhat surprising: it suggests that the desorption of the Li–Mg–N–H system does not follow the same process as Li–N–H, but, more probably, the reported catalytic effects are difficult to reproduce, as the desorption kinetics of the 1:1 LiNH$_2$–LiH mixture are also not improved by catalysts addition in our laboratory.
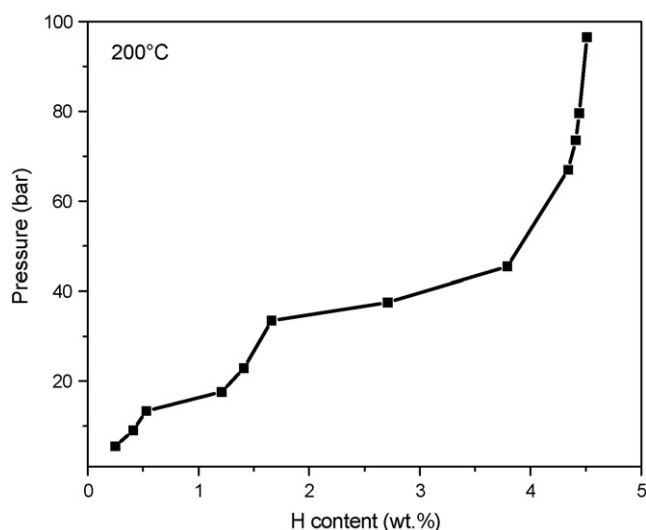
Fig. 8 presents the absorption isotherm obtained at 200 °C for the 12 h ball-milled 1:2 $Mg(NH_2)_2$–LiH mixture, previously outgased at 200 °C under primary vacuum. The isotherm corresponds therefore to the hydrogen absorption of the $Li_2Mg(NH)_2$ phase. The maximum absorption capacity reaches 4.6 wt.% under 100 bar. Surprisingly, two plateaus can be distinguished: one around 15 bar for hydrogen contents between 0.5 and 1.5 wt.% and another one at 38 bar for compositions ranging from 1.5 to 4.5 wt.% of hydrogen. These plateaus are related to biphasic domains and reveal therefore the existence of an intermediate phase. Infrared spectra recorded at different points of the isotherm, thus corresponding to partially rehydrogenated materials, present two doublets: one at 3275 and 3330 cm^{-1} is assigned to the stretching bands of $Mg(NH_2)_2$, which is the expected amide formed upon hydrogenation, and the other doublet (3255 and 3310 cm^{-1}) is more surprisingly similar to that encountered with LiNH$_2$.

These results can be confronted to a recent paper [11], discussing of the possible formation of a $Li_2MgN_2H_3$ phase. Indeed, Luo observed by IR spectroscopy the same coexistence of LiNH$_2$ and $Mg(NH_2)_2$ bands and supposed the formation of a $Li_2MgN_2H_3$ phase, characterized by one NH$_2$ group bonded both to Li and Mg cations. But, conversely to Luo claiming that a solid solution occurs between $Li_2Mg(NH)_2$ and $Li_2MgN_2H_3$, in our case, a plateau is observed on the PCT isotherm, which accounts for a biphasic domain and therefore the existence of a well-defined $Li_2MgN_2H_3$ compound. Further characterizations are currently in progress to better identify this transitory compound.

The 12 h ball-milled 1:2 $Mg(NH_2)_2$–LiH mixture exhibits a nice reversibility at 200 °C with a capacity around 4.8 wt.% after eight cycles (cf. Fig. 9). This gravimetric capacity is the highest reported at 200 °C, as Ti-catalyzed NaAlH$_4$ has a maximum capacity of 3.8–4.0 wt.% at this temperature [4,5]. In spite of the low density of the 1:2 $Mg(NH_2)_2$–LiH mixture (1.18 as measured by liquid pycnometry), we have to emphasize that the

Fig. 8. Absorption isotherm at 200 °C of $Li_2Mg(NH)_2$.
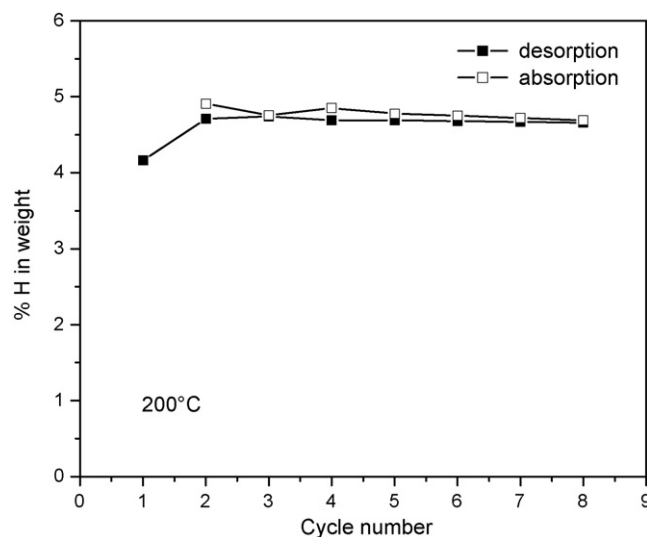
Fig. 9. Storage capacities upon cycling at 200 °C of 12 h ball-milled 1:2 $Mg(NH_2)_2$–LiH as determined by volumetric measurements.

volumetric capacity is rather high: around $56\,\mathrm{g\,dm^{-3}}$ (versus $70\,\mathrm{g\,dm^{-3}}$ for pure liquid hydrogen).

4. Conclusions

The hydrogen storage performances of the Li–Mg–N–H system have been investigated starting either from 1:2 $Mg(NH_2)_2$–LiH or 1:2 MgH_2–LiNH$_2$ mixtures. It has been shown that, for 1:2 MgH_2–LiNH$_2$, the first heating at 200 °C cannot be conducted under a dynamic vacuum, due to the possible ammonia release leading to a fast degradation of the material. This emphasizes the positive role of LiH, if initially present in the mixture, as LiH reacts very quickly with ammonia and avoids the contamination of the hydrogen desorbing flow. The desorption kinetics of the ball-milled 1:2 $Mg(NH_2)_2$–LiH mixture are fast: a total amount of 5.0 wt.% of hydrogen is desorbed in 25 min at 220 °C. The activation energy of desorption process has been estimated around $110\,\mathrm{kJ\,mol^{-1}}$ by both Arrhenius and Kissinger plots. Preliminary results have been given on the structure of the desorbed phase, which is a ternary $Li_2Mg(NH)_2$ imide: this phase crystallizes in a cubic unit cell with a lattice parameter of 10.06(1) Å. The structure is closely related to that of Mg_3N_2 with a fcc stacking of the nitrogen atoms and 3/4 of the tetrahedral sites are occupied by Li and Mg atoms.

In addition, by plotting an absorption isotherm of the $Li_2Mg(NH)_2$ phase at 200 °C, two plateaus have been observed revealing the existence of an intermediary phase between $Li_2Mg(NH)_2$ and the rehydrided material, which is the 1:2 $Mg(NH_2)_2$–LiH mixture. This phase, with a composition close to $Li_2MgN_2H_3$, is characterized by a NH$_2$ group bonded to both Li and Mg atoms as recently reported by Luo and Sickafoose [11].

Regardless of this new phase, we should point out that the 1:2 $Mg(NH_2)_2$–LiH ball-milled material exhibits a nice reversibility at 200 °C with an experimental capacity around 4.8 wt.%. This is the sole material with fast kinetics and such high capacity at 200 °C. This confirms that research on the metal–N–H systems as hydrogen storage materials is very exciting, especially when considering that many other ternary amides or imides have not been investigated yet.

References

[1] G. Sandrock, J. Alloys Compd. 293–295 (1999) 877–888.
[2] F. Cuevas, J.M. Joubert, M. Latroche, A. Percheron-Guégan, Appl. Phys. A 72 (2001) 225–238.
[3] J.J. Reilly, R.H. Wiswall, Inorg. Chem. 7 (1968) 2254–2256.
[4] B. Bogdanovic, M. Schwickardi, J. Alloys Compd. 253–254 (1997) 1–9.
[5] B. Bogdanovic, R.A. Brand, A. Marjanovic, M. Schwickardi, J. Tölle, J. Alloys Compd. 302 (2000) 36–58.
[6] R. Janot, Ann. Chim. Sci. Mater. 30 (2005) 505–517.
[7] P. Chen, Z. Xiong, J. Luo, J. Lin, K.L. Tan, Nature 420 (2002) 302–304.
[8] P. Chen, Z. Xiong, J. Luo, J. Lin, K.L. Tan, J. Phys. Chem. B 107 (2003) 10967–10970.
[9] T. Ichikawa, S. Isobe, N. Hanada, H. Fujii, J. Alloys Compd. 365 (2004) 271–276.
[10] W. Luo, J. Alloys Compd. 381 (2004) 284–287.
[11] W. Luo, S. Sickafoose, J. Alloys Compd. 407 (2006) 274–281.
[12] Z. Xiong, G. Wu, J. Hu, P. Chen, Adv. Mater. 16 (2004) 1522–1525.
[13] Z. Xiong, J. Hu, G. Wu, P. Chen, W. Luo, K. Gross, J. Wang, J. Alloys Compd. 398 (2005) 235–239.
[14] H. Leng, T. Ichikawa, S. Hino, N. Hanada, S. Isobe, H. Fujii, J. Phys. Chem. B 108 (2004) 8763–8765.
[15] T. Ichikawa, K. Tokoyoda, H. Leng, H. Fujii, J. Alloys Compd. 400 (2005) 245–248.
[16] Y. Nakamori, G. Kitahara, S. Orimo, J. Power Sources 138 (2004) 309–312.
[17] S. Orimo, K. Nakamori, G. Kitahara, K. Miwa, N. Ohba, Y. Noritake, S. Towata, Appl. Phys. A 79 (2004) 1765–1767.
[18] J.P. Bohger, R.R. Essmann, H. Jacobs, J. Mol. Struct. 348 (1995) 325–328.
[19] Y. Kojima, Y. Kawai, J. Alloys Compd. 395 (2005) 236–239.
[20] G. Linde, R. Juza, Z. Anorg. Allg. Chem. 409 (1974) 199–214.
[21] R. Juza, K. Opp, Z. Anorg. Allg. Chem. 266 (1951) 325–330.
[22] Y.H. Hu, E. Ruckenstein, J. Phys. Chem. A 107 (2003) 9737–9739.
[23] G. Barkhordarian, T. Klassen, R. Bormann, Scr. Mater. 49 (2003) 213–217.
[24] R. Janot, X. Darok, A. Rougier, L. Aymard, G.A. Nazri, J.-M. Tarascon, J. Alloys Compd. 404–406 (2005) 293–296.
[25] H.E. Kissinger, Anal. Chem. 29 (1957) 1702–1706.
[26] J. Huot, G. Liang, S. Boily, A. Van Neste, R. Schulz, J. Alloys Compd. 293–295 (1999) 495–500.
[27] T. Ichikawa, N. Hanada, S. Isobe, H.Y. Leng, H. Fujii, J. Alloys Compd. 404–406 (2005) 435–438.
[28] S. Isobe, T. Ichikawa, N. Hanada, H.Y. Leng, M. Fichtner, O. Fuhr, H. Fujii, J. Alloys Compd. 404–406 (2005) 439–442.